THE JOURNAL OF BIOLOGICAL CHEMISTRY
Vol. 279, No. 27, Issue of July 2, pp. 27888–27895, 2004

Printed in U.S.A.

Transcriptional Regulation of Rat *CYP2A3* by Nuclear Factor 1

IDENTIFICATION OF A NOVEL NFI-A ISOFORM, AND EVIDENCE FOR TISSUE-SELECTIVE INTERACTION OF NFI WITH THE *CYP2A3* PROMOTER *IN VIVO**[S]

Received for publication, April 2, 2004
Published, JBC Papers in Press, April 28, 2004, DOI 10.1074/jbc.M403705200

Guoyu Ling‡, Charles R. Hauer‡, Richard M. Gronostajski§, Brian T. Pentecost‡, and Xinxin Ding‡¶

From the ‡Wadsworth Center, New York State Department of Health, and School of Public Health, State University of New York, Albany, New York 12201 and the §Department of Biochemistry, State University of New York, Buffalo, New York 14214

Rat *CYP2A3* and its mouse and human orthologs are expressed preferentially in the olfactory mucosa. We found previously that an element in the proximal promoter region of *CYP2A3* (the nasal predominant transcriptional activating (NPTA) element), which is similar to a nuclear factor 1 (NFI)-binding site, is critical for transcriptional activation of *CYP2A3 in vitro*. We proposed that this element might be important for tissue-selective *CYP2A3* expression. The goals of the present study were to characterize NPTA-binding proteins and to obtain more definitive evidence for the role of NFI in the transcriptional activation of *CYP2A3*. The NPTA-binding proteins were isolated by DNA-affinity purification from rat olfactory mucosa. Mass spectral analysis indicated that isoforms corresponding to all four NFI genes were present in the purified NPTA-binding fraction. Further analysis of NPTA-binding proteins led to the identification of a novel NFI-A isoform, NFI-A-short, which was derived from alternative splicing of the NFI-A transcript. Transient transfection assay showed that NFI-A2, an NFI isoform previously identified in the olfactory mucosa, transactivated the *CYP2A3* promoter, whereas NFI-A-short, which lacks the transactivation domain, counteracted the activation. Chromatin immunoprecipitation assays indicated that NFI proteins are associated with the *CYP2A3* promoter *in vivo*, in rat olfactory mucosa, but essentially not in the liver where the *CYP2A3* promoter is hypermethylated and *CYP2A3* is not expressed. These data strongly support a role for NFI transcription factors in the transcriptional activation of *CYP2A3*.

The cytochrome P450 (CYP)[1] superfamily of heme-containing monooxygenases metabolize a wide variety of exogenous as well as endogenous compounds. For example, enzymes of the CYP2A subfamily metabolize xenobiotic compounds such as coumarin, aflatoxin B1, 4-(methylnitrosamino)-1-(3-pyridyl)-1-butanone, nicotine, and cotinine and endogenous compounds such as testosterone, progesterone, and other steroid hormones (1–3). Several members of the *CYP2A* subfamily, including rat *CYP2A3*, mouse *Cyp2a5*, rabbit *CYP2A10*, and human *CYP2A13*, are expressed preferentially in the respiratory tract with the most abundant expression in the olfactory mucosa (OM) (4). The tissue-selective expression of these enzymes is believed to play an important role in the tissue-specific toxicity of numerous xenobiotic compounds in the respiratory tract (1, 4), and a genetic polymorphism of *CYP2A13* has been linked to decreased risks of smoking-related lung adenocarcinoma in humans (5).

The mechanisms that regulate the basal expression and the tissue selectivity of the *CYP2A* genes are not clear. Previously, we identified a conserved DNA element (named the nasal predominant transcriptional activating element, or NPTA element) in the rat *CYP2A3* promoter that interacted with OM-enriched proteins (6). The NPTA element, which is similar to the nuclear factor 1 (NFI)-binding sites (7), was crucial for the activity of the *CYP2A3* promoter *in vitro*. The NPTA-binding proteins have not been fully characterized, but *in vitro* studies showed that at least some of the NPTA-binding complexes are recognized by an antibody to NFI (8).

There are four NFI genes in mammals, NFI-A, -B, -C, and -X, from which numerous NFI isoforms are generated through alternative splicing or alternative promoter usage. NFI proteins are highly conserved in the amino-terminal DNA binding/dimerization domains, whereas the carboxyl termini contain diverse transactivation/repression domains (7). NFI isoforms are thought to be involved in the regulation of developmental and tissue-specific gene expression (7, 9, 10). Recent studies using knockout mouse models have demonstrated that the NFI genes play important roles in the development of tissues such as brain, lung, and tooth (11–13). The expression of the NFI genes in the OM has been studied using molecular cloning and *in situ* hybridization; all four NFI genes are expressed in the OM (14, 15). However, the identities of the specific isoforms have not been determined, with the exception of NFI-A2, which is a recently identified NFI isoform that is detected in the OM (14, 16). Most interesting, we found that NFI-A2 was capable of activating a reporter construct containing the NPTA element in yeast one-hybrid assays (16).

In the present study, we used DNA-affinity chromatography to isolate the *CYP2A3* NPTA-binding proteins from rat OM for identification by immunoblot and mass spectral (MS) analyses. These efforts have confirmed NFI as the major NPTA-binding proteins and have led to the identification of a novel NFI-A

* This work was supported in part by United States Public Health Service Grant ES07462 (to X. D.), DK58401, and HD34908 (to R. M. G.). The costs of publication of this article were defrayed in part by the payment of page charges. This article must therefore be hereby marked "*advertisement*" in accordance with 18 U.S.C. Section 1734 solely to indicate this fact.

[S] The on-line version of this article (available at http://www.jbc.org) contains additional Experimental Procedures and Refs. 1–4.

¶ To whom correspondence should be addressed: Wadsworth Center, New York State Department of Health, Empire State Plaza, Box 509, Albany, NY 12201-0509. Tel.: 518-486-2585; Fax: 518-486-1505; E-mail: dingx@wadsworth.org.

[1] The abbreviations used are: CYP, cytochrome P450; OM, olfactory mucosa; MS, mass spectral; EMSA, electrophoretic mobility shift assays; RT, reverse transcription; NFI, nuclear factor 1; ChIP, chromatin immunoprecipitation; NPTA, nasal predominant transcriptional activating; PBS, phosphate-buffered saline; PIPES, piperazine-1,4-bis(2-ethanesulfonic acid); PMSF, phenylmethanesulfonyl fluoride; IP, immunoprecipitation; BisTris, 2-[bis(2-hydroxyethyl)amino]-2-(hydroxymethyl)propane-1,3-diol.

isoform, named NFI-A-short, that has a truncated transactivation/repression domain. The tissue distribution of NFI-A-short and the levels of NFI-A2, NFI-A-short, and total NFI-A mRNAs were determined by reverse transcription (RT)-PCR, and the functions of the two NFI-A isoforms at the *CYP2A3* promoter were analyzed by using transient transfection assays in cultured mammalian cells. Furthermore, chromatin immunoprecipitation (ChIP) assays using rat liver and OM tissues demonstrated a tissue-selective association of NFI with the *CYP2A3* promoter *in vivo*. In addition, the methylation status of the *CYP2A3* promoter region in these two tissues was also compared, so as to derive a better understanding of the mechanistic basis of the tissue-specific interaction of the promoter with NFI. These studies provide compelling evidence for the *in vivo* role of NFI transcription factors in the expression of *CYP2A3*.

EXPERIMENTAL PROCEDURES

Nuclear Extract Preparation and Electrophoretic Mobility Shift Assays (EMSA)—Heads of adult male Wistar rats (Harlen Bioproducts) were frozen in liquid nitrogen immediately after decapitation. Frozen rat heads were partially thawed at 4 °C before dissection of OM. Nuclear extract was prepared according to the protocol of Kudrycki *et al.* (17). EMSA was performed as described previously, with a double-stranded NPTA element (6).

Reporter Plasmid Construction, Cell Culture, Transfection, and Luciferase Reporter Assays—For the preparation of the *CYP2A3*-luciferase reporter gene construct, a 254-bp *CYP2A3* proximal promoter region (−254 to +1), with either a wild-type (pGL2A3) or a mutated (pGL2A3M) NPTA element (6), was inserted into the pGL3-Basic vector (Promega). Expression vectors for NFI-A2 (pNFI-A2) and NFI-A-short (pNFI-A-short) were modified from the pCHNFI-A1.1 vector that has a cytomegalovirus promoter and the mouse NFI-A1 coding sequence (9). pNFI-A2 was prepared by replacement of the NFI-A1 sequence with NFI-A2, as a 1.6-kb NotI-KpnI fragment (16). pNFI-A-short was generated by replacement of the EcoRV-KpnI fragment of NFI-A1 with an ~600-bp EcoRV-KpnI fragment of NFI-A-short; the mouse NFI-A1 sequence (NotI-EcoRV) that remained in the vector encodes the same amino acids as in rat NF1-A1. A vector with no NFI insert (pCMV), used as a control, was prepared by modification of pCHNFI-A1.1. All constructs were sequenced for confirmation of structural integrity.

Human choriocarcinoma JEG-3 cells (HTB-36, ATCC) were cultured at 37 °C in Dulbecco's modified Eagle's medium, supplemented with 10% fetal bovine serum, 2 mM glutamine, 100 units/ml penicillin, and 0.1 mg/ml streptomycin (Sigma). Firefly luciferase reporter gene constructs, NFI expression constructs, and a *Renilla* luciferase construct pRL-SV40 (Promega) were co-transfected into JEG-3 cells with use of LipofectAMINE 2000 (Invitrogen), according to the manufacturer's instructions. Transfections were done in duplicate using at least two different DNA preparations. Cells were harvested 48 h after transfection. The Dual Luciferase Reporter Assay System (Promega) was used for determination of the relative luciferase activities. Luminescence was measured using a luminometer (LB9501, Berthold). For each sample, the activity of the firefly luciferase was normalized by that of the *Renilla* luciferase.

Chromatin Immunoprecipitation Assay—ChIP was performed as described (18), with modifications. Approximately 1 g of freshly dissected rat liver or OM from four rats was used for the preparation of chromatin. Tissues were minced on ice and transferred to 20 ml of Dulbecco's modified Eagle's medium in a 50-ml tube, to which formaldehyde was added to a final concentration of 1% (v/v), for cross-linking of proteins to DNA. The mixture was incubated at room temperature for 15 min with constant rocking. Reactions were stopped by the addition of 0.125 M glycine. The tissues were collected by a brief spin, washed with ice-cold phosphate-buffered saline, and homogenized in 4 ml of phosphate-buffered saline containing a protease inhibitor mixture (1836153, Roche Applied Science) using a Dounce homogenizer (type A pestle, 10 strokes). The dissociated cells were filtered through four layers of cheesecloth, transferred to microcentrifuge tubes, and collected by spinning at 2000 × *g* for 10 min. Cells were washed with RSB buffer (10 mM Tris-HCl, pH 7.5, containing 10 mM NaCl, 3 mM $MgCl_2$, supplemented with the Roche Applied Science protease inhibitor mixture) and were incubated with cell lysis buffer (5 mM PIPES buffer, pH 8.0, containing 85 mM KCl, 0.5% Nonidet P-40, supplemented with the protease inhibitor mixture from Roche Applied Science) for 10 min at 4 °C. After incubation, the nuclei were collected by centrifugation and were resuspended in 500 μl of immunoprecipitation (IP) buffer (25 mM Tris-HCl, pH 8.0, containing 2 mM EDTA, 150 mM NaCl, 1% Triton X-100, 0.1% SDS, 2.5 mM PMSF, and the protease inhibitor mixture (Roche Applied Science)) in 1.5-ml microcentrifuge tubes. About 0.1 g of glass beads (G-1277, Sigma) were added to each tube, and the nuclei were sonicated on ice 20 times for 15 s each time, at 30% of maximum power, with a VibraCell ultrasonic processor (600 watts) equipped with a microtip (Sonics & Materials). Fragmented chromatin was separated from the glass beads and intact nuclei by centrifugation at 12,000 × *g* for 15 min at 4 °C. Aliquots of chromatin suspension were stored at −80 °C until use.

Sonicated chromatin, equivalent to ~60 mg of tissue for each tube, was diluted to 1.5 ml with the IP buffer and was mixed at 4 °C for 2 h with 0.1 ml of protein A-Sepharose (Amersham Biosciences) that had been pretreated with 0.4 mg/ml sonicated salmon sperm DNA and 1 mg/ml bovine serum albumin. After a brief centrifugation, two 0.7-ml aliquots of the supernatant were transferred to two new tubes, which were incubated overnight on a rotating platform with 3 μg of either normal rabbit IgG or the anti-NFI antibody H300 (both from Santa Cruz Biotechnology). The H300 antibody is against the conserved amino-terminal half of an NFI protein. The mixtures were then incubated with 30 μl of protein A-Sepharose at 4 °C for 2 h, followed by a brief centrifugation. An aliquot of the supernatant from the samples incubated with normal IgG was saved as the "input" chromatin. The pellets were washed twice with 1.4 ml of wash buffer I (50 mM Tris-HCl, pH 8.0, containing 2 mM EDTA, 0.2% Sarkosyl, and 1 mM PMSF) and four times with 1.4 ml of wash buffer II (100 mM Tris-HCl, pH 9.0, containing 500 mM LiCl, 1% Nonidet P-40, 1% deoxycholic acid, and 1 mM PMSF). The immobilized immune complexes were dissociated by incubating twice in 250 μl of elution buffer (0.1 M $NaHCO_3$ and 1% SDS) at room temperature for 15 min each. The cross-link was subsequently reversed by addition of NaCl to the eluted fractions to a final concentration of 300 mM and then heating at 68 °C for 6 h in the presence of 20 μg/ml RNase (Roche Applied Science, catalog number 1579681). DNA was then precipitated by ethanol, resuspended in 100 μl of PK buffer (10 mM Tris-HCl, pH 7.5, containing 5 mM EDTA, 0.25% SDS, and 20 μg of proteinase K), and after a 1-h incubation at 45 °C, purified using QIAquick columns (Qiagen).

RT-PCR—Real time quantitative PCR was performed using a LightCycler and the LightCycler FastStart DNA Master SYBR Green I kit (Roche Applied Science). The reaction mixtures contained 2 μl of DNA templates, 1.5 mM $MgCl_2$, 0.5 μM each of the primers, and 1 μl of 1× DNA Master SYBR Green I in a total volume of 10 μl. The following primers were used to quantitate the promoter fragments in immunoprecipitated samples: for *CYP2A3*, 5′-tccctgttaatctgtcatggag-3′ and 5′-tgggatgacagacacagtga-3′, amplifying −169 to +16 of the *CYP2A3* promoter; for *CYP1A2*, 5′-tggaactgagggatcatggctt-3′ and 5′-aagctaaggtgggtccctgttt-3′, amplifying −142 to +140 of the *CYP1A2* promoter; and for immunoglobulin-β (IgB), 5′-ttcaagtcctagcagaccag-3′ and 5′-agggtctggggcaaaacatg-3′, amplifying −173 to +5 of the IgB promoter (19). The CYP2A3 and CYP1A2 PCR products include NFI-like elements, whereas the IgB PCR product (used as a negative control) does not. The annealing temperature for these primer pairs was 65 °C. Cycle numbers were used for calculation of the amounts of specific DNA sequences in the immunoprecipitated samples, relative to the amounts present in total input, as described previously (20). Standard curves for quantitation were generated from serial dilutions of the input chromatin. Fold enrichment of a promoter fragment is the fold difference between its amount in the NFI antibody-precipitated DNA and its amount in the control IgG-precipitated DNA.

Restriction Analysis of DNA Methylation—Genomic DNA from rat OM and liver (50 μg each) was digested overnight with SacI and PvuII, 250 units each, in a total volume of 100 μl. After confirmation of complete digestion, the DNA was precipitated by ethanol and was resuspended in water. The resuspended DNA was then divided into two aliquots, which were incubated overnight with 200 units of either HpaII (methylation-sensitive) or MspI (methylation-insensitive). After digestion, the enzymes were inactivated by heating at 65 °C, for 20 min, and the DNA fragments were detected on Southern blots, with a 2070-bp SacI-PvuII *CYP2A3* promoter fragment as the probe.

Other Methods—For SDS-PAGE, proteins were separated in 10% BisTris NuPage gels, according to the manufacturer's instruction (Invitrogen), and detected using a Colloidal Blue kit or a SilverQuest silver staining kit from Invitrogen. Western blot analysis was carried out using an ECL reagent (Amersham Biosciences), with use of the anti-NFI antibody (H300). RNA was prepared from adult Wistar rats (Charles River Breeding Laboratories), with use of TRIzol reagent (Invitrogen). A 3′-rapid amplification of cDNA end kit (Invitrogen) was

used to clone the putative, short NFI isoforms, with an NFI-A gene-specific primer (5′-ctgatggtgaacgccttgtg-3′) and the universal amplification primer. PCR products were gel-purified and then cloned into the TOPO XL vector (Invitrogen). Experimental procedures for the purification and MS analysis of NPTA-binding proteins and methods for RT-PCR quantification of NFI-A mRNAs are described in the Supplemental Material.

RESULTS

Purification and Identification of NPTA-binding Proteins—We developed a two-step DNA-affinity chromatography scheme to identify proteins that bind to the NPTA element of *CYP2A3* in rat OM. A DNA fragment containing 12 copies of the NPTA element was prepared and was used to generate NPTA-Sepharose and NPTA-Dynabead. Nuclear extract (~100 mg of total protein, from ~200 rat heads) was fractionated on a 1-ml NPTA-Sepharose column; bound proteins were eluted by increasing the KCl concentration stepwise, in 100 mM increments. Column fractions were analyzed for NPTA binding activity by EMSA. The highest activity was found in the 0.6 M KCl fraction (Fig. 1*A*). Additional clean-up steps before the NPTA-Sepharose column, either anion-exchange or cation-exchange column chromatography, did not improve yield (data not shown). Proteins in the 0.5–0.7 M KCl fractions were pooled and dialyzed to remove KCl and were further purified using NPTA-Dynabeads. Strong NPTA binding activity was recovered in the 0.6 M NaCl fraction (Fig. 1*B*). This fraction contained numerous proteins, most of which had molecular masses between 20 and 50 kDa (Fig. 1*C*).

The sequence of the NPTA element is similar to sequences of known NFI-binding sites. Therefore, we suspected that the affinity-purified NPTA-binding proteins contain multiple NFI isoforms. Indeed, NFI proteins were highly enriched in the 0.6 M NaCl fraction, as indicated by Western blot analysis using an anti-NFI antibody that recognizes all NFI isoforms (Fig. 1*D*).

Proteins encoded by each of the four NFI genes were detected in the affinity-purified fractions, as indicated by the presence of peptides unique to each gene (Table I), although the peptides detected did not permit the distinction among specific NFI proteins of each type (such as NFI-A1 and NFI-A2). However, data from MS analysis did not indicate the presence of any other known transcription factors, which suggested that the NFI proteins are the major NPTA-binding proteins. Furthermore, the relative abundance of the unique NFI-A peptides was 2–8-fold greater than the abundance of peptides of the other NFI proteins in three independent experiments (data not shown), suggesting that, in rat OM, NFI-A is the most abundant among the four types of NFI proteins. Also of note, various peptides derived from NFI-A were found with either unmodified or phosphorylated serines at residues 191 and 193. Moreover, all of the NFI-related peptides identified in the affinity-purified fractions were from the 30-kDa NH_2-terminal half of full-length NFI proteins, as shown in Fig. 1*E* for peptides that correspond to an NFI-A isoform.

Identification of A Novel NFI-A Isoform That Contains Truncated Activation/Repression Domain—The absence of any peptides corresponding to the carboxyl-terminal portion of the identified NFI proteins suggested that proteolysis was occurring during purification, although efforts had been made to minimize protein degradation. However, this finding also suggested the possible occurrence of unidentified, shorter NFI isoform(s) corresponding to the ~30-kDa proteins detected by SDS-PAGE and Western blot analysis of both the purified fraction and OM nuclear extract. NFI isoforms with truncated carboxyl-terminal activation/repression domains have been reported in other species (7, 21). To detect mRNAs encoding putative, short NFI isoforms, we performed 3′-rapid amplification of cDNA end experiments with rat OM RNA and primers

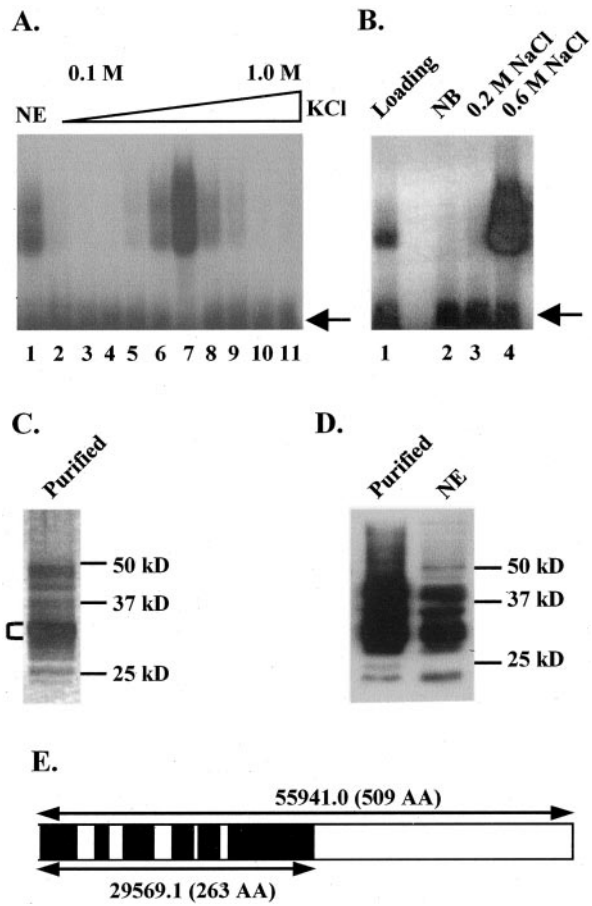

FIG. 1. **Purification and identification of NPTA-binding proteins from rat OM.** *A*, EMSA analysis of fractions eluted from an NPTA-Sepharose DNA affinity column. Nuclear extract (~100 mg of protein at ~1.3 mg of protein/ml) from OM of adult rats was applied to a 1-ml NPTA-Sepharose column. *Lane 1,* nuclear extract (*NE*); *lanes 2–11*, fractions eluted with 0.1–1.0 M KCl at 100 mM increments (~1 ml each). EMSA was performed with labeled NPTA element, using 5 μl of nuclear extract or eluted fraction. *Arrow* indicates the position of the free probe. *B*, EMSA analysis of fractions eluted from NPTA-Dynabead. Fractions containing NPTA binding activity from the NPTA-Sepharose column were pooled (~3 ml total) and were further purified with 100 μl of NPTA-Dynabeads. *Lane 1,* pooled fractions from the NPTA-Sepharose column (*Loading*); *lane 2*, non-bound fraction (*NB*); *lanes 3* and *4*, fractions eluted with 0.2 or 0.6 M NaCl (about 30 μl each). EMSA was performed using 2 μl of each fraction. *C* and *D*, approximately one-third of the affinity-purified NPTA-binding proteins (*Purified*) were analyzed on SDS-PAGE and visualized by silver stain (*C*) or by immunoblotting using an anti-NFI antibody (*D*). A sample of OM nuclear extract (*NE*, 5 μg) was also analyzed on the immunoblot. The positions of selected (prestained) protein size markers (Bio-Rad catalog number 161-0362) are indicated. *E*, identification of NFI-A by MS analysis of affinity-purified NPTA-binding proteins. The most prominent bands (~30 kDa, *C*) on a Coomassie Blue-stained SDS-PAGE gel were used for in-gel tryptic digestion and MS analysis, as described under "Experimental Procedures." *Dark boxes* represent locations where sequence matches were found between identified tryptic peptides and rat NFI-A1 protein. The predicted mass and total number of amino acids (*AA*) for NFI-A1 (*top*) and the putative OM NFI-A protein (*bottom*) are shown. Protein coverage (against NFI-A1): 39.7% (202:509) by amino acid count, 39.6% by mass.

specific for NFI-A. Several cDNA clones with sequences corresponding to a novel, short NFI-A isoform (designated NFI-A-short; GenBank™ accession number AY572794) were isolated. A full-length NFI-A-short cDNA (~0.9 kb) was subsequently obtained by RT-PCR, using OM RNA as template, with a primer corresponding to the 5′-end of NFI-A1 (GenBank™ accession number D78017) and an NFI-A-short-specific primer, derived from the putative 3′-untranslated region of the short mRNA. A comparison of the cDNA sequence of NFI-A-short

TABLE I
NFI gene-specific peptides detected in affinity-purified NPTA-binding proteins of rat OM

Gene	GenBank™ accession number	NFI gene-specific peptides detected by MS analysis
NFI-A	BAA11203	AVKDELLSEKPEVK, DELLSEKPEVK, DIRPEYREDFVLTVTGK
NFI-B	AAF23586	AVKDELLSEKPEIK
NFI-C	AAF23587	EDFVLAVTGK, APGCVLSNPDQK, FVLAVTGK
NFI-X	BAA25295	AVKDELLGEKPEIK, DIRPEFR, EDFVLTITGK

with that of NFI-A1 revealed that the two sequences are identical, except that in NFI-A-short exon 5 was spliced to an alternative exon 6 (Fig. 2*A*), which encodes three amino acids followed by a stop codon (Fig. 2*B*). The resulting NFI-A-short protein (about 31 kDa) has an intact DNA binding and dimerization domain (encoded by exon 2) but lacks most of the transactivation/repression domain.

Tissue distribution of NFI-A-short mRNA was determined using RT-PCR, with a forward primer derived from exon 5, and a reverse primer that is unique for NFI-A-short mRNA. The PCR product representing NFI-A-short mRNA (~250 bp) was detected in RNA preparations from all rat tissues examined, including OM, lung, liver, brain, and kidney (Fig. 2*C*). In experiments not shown, the same primer pair amplified a 1.1-kb fragment from rat genomic DNA. This 1.1-kb PCR product contained an 865-bp intron sequence flanked by exons 5 and 6 of NFI-A-short. A comparison of the sequence of this PCR product with that of the rat NFI-A genomic sequence (GenBank™ accession number NW_043856) indicated that the new exon 6 in NFI-A-short is located at ~5 kb upstream of the original exon 6 of the NFI-A gene (Fig. 2*A*). We did not detect a similar NFI-A-short in mice (data not shown), which indicated that this alternative splicing may be specific for rats.

The relative mRNA levels of total NFI-A, NFI-A2, and NFI-A-short in rat OM, liver, lung, brain, and kidney were determined by using real time quantitative RT-PCR, with gene-specific or isoform-specific primers. As shown in Table II, of the five tissues, liver had the highest and lung had the lowest levels of total NFI-A mRNA. The expression level of NFI-A-short was low in all tissues examined (~0.5–2% of total NFI-A mRNA). NFI-A2, which had been shown previously (16) to be enriched in the OM, accounted for 2.7% of total NFI-A mRNA and was about twice as abundant as NFI-A-short in OM. The presumed low abundance of NFI-A-short and NFI-A2 proteins in the OM is consistent with our failure to detect the unique carboxyl-terminal tryptic peptide of NFI-A-short and the unique amino-terminal tryptic peptide of NFI-A2 by MS analysis of total peptides derived from the affinity-purified OM NPTA-binding proteins.

NFI-A2 and NFI-A-short Form Homo- and Heterodimers When Bound to the CYP2A3 Promoter—We transfected human choriocarcinoma JEG-3 cells with plasmids containing NFI-A2 or NFI-A-short cDNA to characterize further the abilities of NFI-A2 and NFI-A-short to bind to the NPTA element and the potential interactions between the two NFI proteins. The expression of NFI protein and the presence of NPTA binding activity in transfected cells were determined by immunoblot analysis (using an antibody that reacts with all NFI proteins) and by EMSA (using ^{32}P-labeled NPTA element), respectively. Extracts of mock-transfected JEG-3 cells had low endogenous NFI proteins (Fig. 3*A*), and they had no detectable NPTA binding activity (Fig. 3*B*). NFI-A2 and NFI-A-short proteins were easily detected following transient transfection, and they had the following expected sizes: ~30 kDa for NFI-A-short and ~57 kDa for NFI-A2 (Fig. 3*A*). NPTA binding activities were detected in extracts of either NFI-A2-transfected or NFI-A-short-transfected JEG-3 cells. As expected, the size of the NPTA-binding complex was smaller for NFI-A-short-transfected cells than for NFI-A2-transfected cells (Fig. 3*B*). However, a complex of intermediate size as well as the two complexes detected in the respective singly transfected cells were found in incubations with extracts from cells co-transfected with NFI-A2 and NFI-A-short. The appearance of the intermediate-sized complex was accompanied by decreases in the intensities of the other two bands (Fig. 3*B*). Yet the expression level of each of the NFI proteins was comparable in the co-transfected and in the respective singly transfected cells (Fig. 3*A*). These results indicate that NFI-A2 and NFI-A-short can bind to the NPTA element *in vitro* as a heterodimer, as well as a homodimer.

Differing Effects of NFI-A2 and NFI-A-short on the Activity of CYP2A3 Promoter—The abilities of NFI-A2 and NFI-A-short to activate the *CYP2A3* promoter were tested using a reporter gene system. A 254-bp *CYP2A3* promoter, containing either the wild-type NPTA element or a mutated NPTA element that cannot form complexes with NPTA-binding proteins (6), was cloned into pGL3-Basic vector to give pGL2A3-Luc and pGL2A3M-Luc, respectively. The reporter constructs and NFI expression vectors were co-transfected into JEG-3 cells. Transfection with NFI-A2 activated the expression of pGL2A3-Luc in a dose-dependent manner, whereas transfection with NFI-A-short had no effect on pGL2A3-Luc expression (Fig. 4*A*). The effects of NFI-A2 were dependent on its binding to the NPTA element, as activation of pGL2A3M-Luc was not observed (Fig. 4*A*). Most interesting, co-transfection with NFI-A-short and NFI-A2 led to an ~40% inhibition of pGL2A3-Luc expression, as compared with transfection with NFI-A2 alone (Fig. 4*B*); no similar inhibitory effect was observed when pCMV was used in place of pNFI-A-short (data not shown). The residual pGL2A3-Luc expression was still substantial, suggesting that the heterodimer of NFI-A2 and NFI-A-short is still functional, albeit less effective.

Interaction of NFI with the CYP2A3 Promoter in Vivo—The ability of NFI proteins to bind to the NPTA element *in vitro* does not necessarily prove that the same proteins are bound to the NPTA elements *in vivo*, in a given tissue or cell type, since access to DNA-binding sites may be influenced by such factors as chromatin structure, occupancy of the binding sites by other DNA-binding proteins, and intranuclear availability of the NFI proteins. To determine whether NFI proteins interact with the *CYP2A3* promoter *in vivo*, in a tissue-specific fashion, we performed ChIP assays. Because a cell line with *CYP2A3* expression has not been identified, we performed the ChIP assays with rat OM and liver. *CYP1A2* was used as a positive control. Unlike *CYP2A3*, which is not expressed in liver, *CYP1A2* is abundantly expressed in both OM and liver. An NFI-like element is present in the *CYP1A2* promoter; *in vivo* occupancy of this element in rat liver, presumably by NFI-related transcription factors, had been demonstrated by *in vivo* DNase I footprinting assays (8). An anti-NFI antibody, which has been shown to immunoprecipitate NFI proteins derived from all four NFI genes (22), was used to enrich NFI-associated DNA sequences. The levels of the *CYP2A3* NPTA element and the *CYP1A2* NFI-binding site were quantitated using real time PCR in the DNA fragments pulled down by the anti-NFI antibody and were compared with their levels in the nonspecific

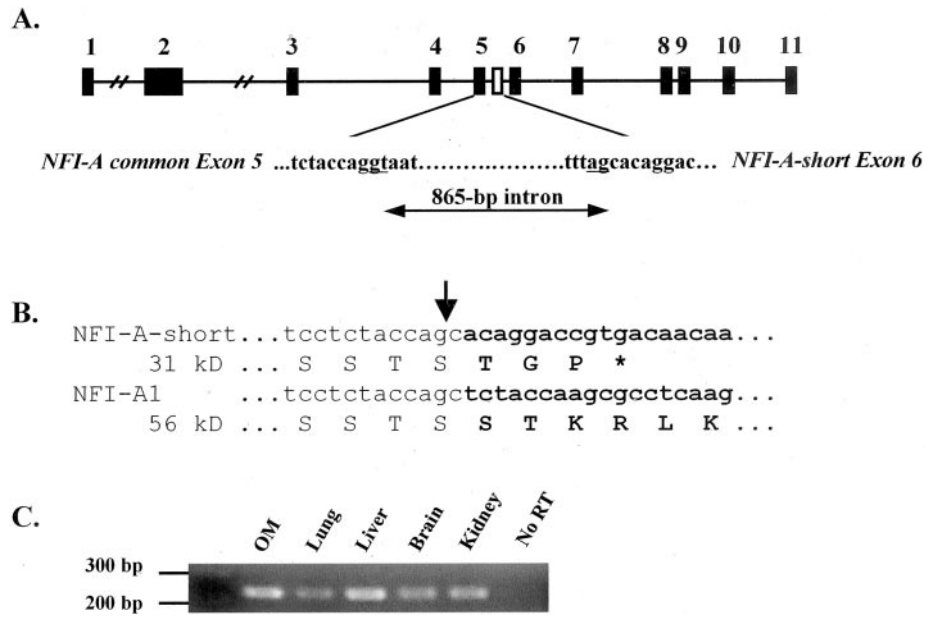

FIG. 2. **Structure and tissue distribution of NFI-A-short.** *A*, structure of the NFI-A gene and location of alternative splicing for NFI-A-short. Common NFI-A exons are shown as *black boxes* and are numbered on *top*. The predicted alternative exon 6 in NFI-A-short (at 865 bp downstream of the NFI-A common exon 5) is shown as an *open box.* Putative splicing donor and acceptor sequences are *underlined*. *B*, partial cDNA and deduced amino acid sequences of NFI-A-short and NFI-A1. Sequences that differ between the two are shown in *boldface.* The new exon 6 of NFI-A-short encodes three amino acids and a stop codon (*), which would result in an ~31-kDa protein. *Arrow* indicates putative splicing site. *C*, detection of NFI-A-short mRNA in various rat tissues by RT-PCR. Reverse transcriptase was omitted in negative control reactions (*No RT*). The positions of selected fragments of a 100-bp DNA ladder are shown.

TABLE II
Quantitative analysis of NFI-A mRNA expression in various rat tissues

Total RNA preparations from various tissues of adult female Wistar rats were used for quantitative RT-PCR analysis using primers common for all NFI-A isoforms as well as primers specific for NFI-A-short or NFI-A2. Levels of the various NFI transcripts were normalized to the level of β-actin mRNA in each sample. Data presented are means ± S.D. (n = 3).

Tissue	Total NFI-A	NFI-A-short	NFI-A2
		copy number per 10^3 copies of β-actin	
OM	27 ± 2	0.35 ± 0.05	0.72 ± 0.04[a]
Liver	60 ± 17	0.59 ± 0.15	ND[b]
Brain	30 ± 7	0.15 ± 0.02	ND
Lung	7.7 ± 0.4	0.07 ± 0.01	ND
Kidney	14 ± 4	0.29 ± 0.10	ND

[a] Significantly higher than NFI-A-short; $p < 0.01$.
[b] ND, not determined and not detected in a previous study (16).

DNA fragments pulled down by a control antibody (normal IgG). The proximal region of the IgB promoter, which does not contain an NFI-binding site, was used as an additional negative control for antibody specificity. PCR cycle numbers for these samples ranged from 28 to 34 and were inversely proportional to the DNA log concentration (data not shown). For OM, IP with the anti-NFI antibody led to moderate enrichments of both *CYP2A3* (5.2 ± 1.6-fold; n = 4) and *CYP1A2* promoters (5.3 ± 1.4-fold; n = 4) (Fig. 5*A*). On the other hand, for liver, IP with the anti-NFI antibody led to a strong enrichment of the *CYP1A2* promoter (11 ± 5.4-fold; n = 4) but only a <2-fold (1.8 ± 0.7; n = 4) enrichment of the *CYP2A3* promoter (Fig. 5*B*). No enrichment of the IgB promoter was observed in either tissue. These data strongly suggest that in the OM NFI proteins are associated with the *CYP2A3* and *CYP1A2* promoters *in vivo*, whereas in the liver, NFI proteins, although present, have little interaction with the *CYP2A3* promoter *in vivo*.

Differential Cytosine Methylation at the CYP2A3 Promoter in OM and Liver—Data from the ChIP assays suggested potential tissue differences in chromatin accessibility at the *CYP2A3* promoter; such tissue differences may be at least partly due to differential CpG methylation, and such methylation is known to be correlated with closed chromatin state and gene silencing in a tissue-specific manner (23). Therefore, we determined the cytosine methylation status in the proximal region of the *CYP2A3* promoter (Fig. 6*A*), using a methylation-sensitive restriction enzyme and Southern blot analysis (Fig. 6*B*). Complete digestion of genomic DNA, isolated from rat liver (Fig. 6*B*, *lanes 1* and *2*) and OM (Fig. 6*B*, *lanes 3* and *4*), first with SacI and PvuII and then with MspI, gave rise to four small fragments, 240, 453, 609, and 768 bp (Fig. 6*B*, *lanes 1* and *3*), as predicted from the restriction map (Fig. 6*A*). However, when MspI was replaced with its methylation-sensitive isoschizomer HpaII, none of the four small bands was detected in the liver DNA sample (Fig. 6*B*, *lane 2*). Instead, the *CYP2A3* promoter was detected as the uncut 2070-bp SacI-PvuII fragment and a minor band derived from a partial digest by HpaII. In contrast, the four small fragments were still detected in HpaII-digested OM DNA samples (Fig. 6*B*, *lane 4*), albeit in lower amounts than for MspI-digested samples. However, the uncut 2070-bp SacI-PvuII fragment and other fragments partially cut by HpaII were abundant in the OM DNA samples, implicating methylation of the *CYP2A3* promoter in a significant number of cells of the OM. Thus, the CpG sites within the HpaII recognition sequence in the *CYP2A3* promoter were heavily methylated in the liver, but they were hypomethylated in at least some of the cells of the OM.

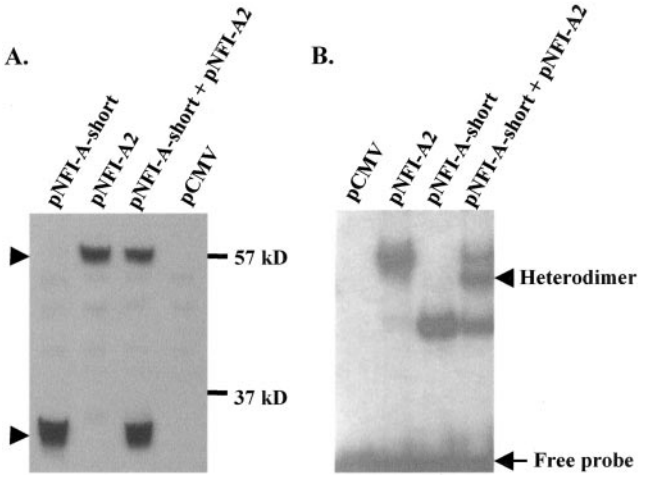

FIG. 3. **NFI-A2 and NFI-A-short bind to the NPTA element as homo- and heterodimers.** *A*, heterologous expression of NFI-A2 and NFI-A-short in JEG-3 cells. JEG-3 cells cultured in 100-mm plates were harvested 48 h after transient transfection with the indicated NFI-A cDNA expression vectors (10 μg each). Control transfection was performed with pCMV vector. About 5 μg of whole-cell extracts were used for immunoblot analysis with an anti-NFI antibody (H300). The positions of selected (prestained) protein size markers (Bio-Rad catalog number 161-0318) are indicated. *Arrowheads* indicate NFI proteins of predicted sizes. *B*, EMSA was carried out using a radiolabeled NPTA probe and the whole-cell extracts described in *A*. The *arrow* indicates position of free probe, and the *arrowhead* indicates NFI-A2/NFI-A-short heterodimer.

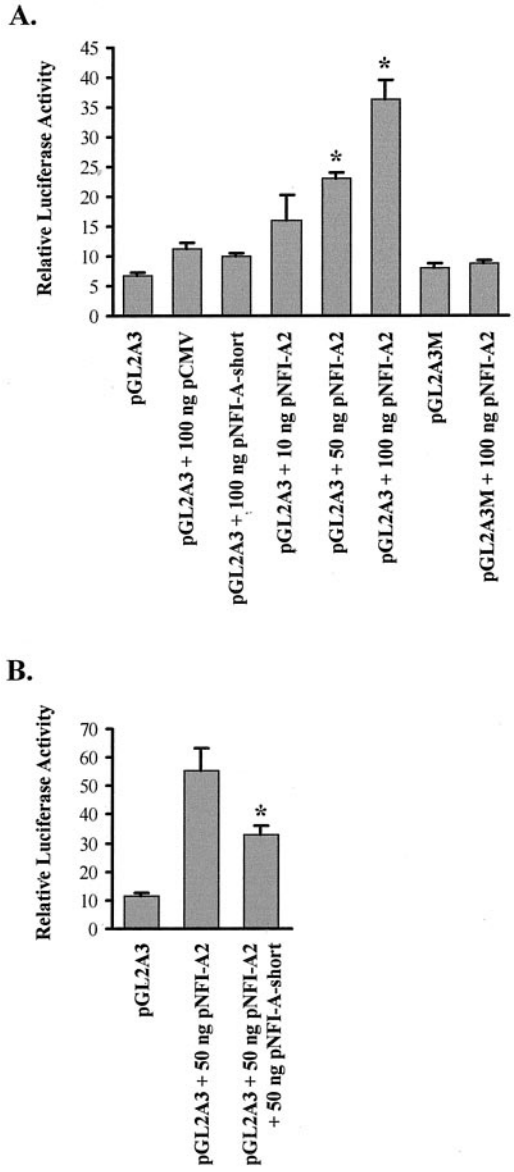

FIG. 4. **Effects of NFI proteins on *CYP2A3* promoter activity.** *A*, activation of *CYP2A3* promoter by NFI-A2, but not by NFI-A-short. JEG-3 cells grown in 6-well plates were co-transfected with pCMV (vector control), pNFI-A2, or pNFI-A-short at indicated amounts; 10 ng of pRL-SV40 *Renilla* luciferase vector (internal control); and 2 μg of pGL2A3 or pGL2A3M (reporter construct). In pGL2A3, the firefly luciferase cDNA is driven by a wild-type 254-bp *CYP2A3* promoter. pGL2A3M differs from pGL2A3 by a *tg* to *gt* mutation, within the NPTA element, that abolishes NFI binding. Activities of firefly luciferase in cell lysates were normalized by those of *Renilla* luciferase, and the relative activities are expressed in arbitrary units (means ± S.D., n = 4). *, significantly different from vector control; $p < 0.01$. *B*, NFI-A-short inhibits the activity of NFI-A2 at the *CYP2A3* promoter. JEG-3 cells were transfected with pNFI-A2 or both pNFI-A2 and pNFI-A-short, at indicated amounts, together with pRL-SV40 and pGL2A3 in the amounts described in *A*. *, significantly lower than the activities in cells transfected with pNFI-A2 alone; $p < 0.01$.

DISCUSSION

Many *CYP*s are tissue-selectively expressed in mammals, but little is yet known of the mechanisms of their tissue specificity. Several recent studies (6, 8, 16, 24) have explored the mechanisms of the respiratory tract-selective expression of the *CYP2A* and *CYP2F* genes. A putative lung-specific factor was identified that bound to human *CYP2F1* proximal promoter region and potentially activated its lung-selective expression (24). For *CYP2A*s, we had identified previously an NFI-like element (NPTA element) within the proximal promoter region of the rat *CYP2A3* by gel-shift and footprinting assays and had demonstrated a potential role of this element in the tissue-selective expression of *CYP2A3* via a number of *in vitro* approaches, including *in vitro* transcription and Southwestern assays (6). We also obtained evidence from supershift assays that at least some of the NPTA-binding proteins can be recognized by an antibody to NFI (6, 8). However, definitive evidence for the identity of the NPTA-binding proteins and for their *in vivo*, tissue-selective interaction with the *CYP2A3* NPTA element was not obtained. In the present study, a two-step DNA affinity chromatography scheme was developed to enable purification of the NPTA-binding proteins from the nuclear extract of rat OM for MS analysis. We now have definitive evidence that the OM NPTA-binding proteins include all four types of NFI factors. We have also identified a novel rat NFI isoform (NFI-A-short) in the OM, and we demonstrate that it acts as a suppressor of the transcriptional activation of a *CYP2A3*-luciferase reporter gene by NFI-A2 in co-transfection assays. More important, by using a tissue-based ChIP assay, we have shown that the *CYP2A3* NPTA element is bound by NFI factors *in vivo* in the OM but essentially not in the liver. These data not only provide strong support for the *in vivo* function of NFI proteins in the tissue-selective expression of *CYP2A3* in the OM, but they also illustrate, for the first time, the feasibility of performing ChIP assays on the OM.

NFI transcription factors bind as dimers to the consensus sequence TTGGC(N_5)GCCAA on duplex DNA (7). Although NFI genes are ubiquitously expressed, distinct NFI isoforms can be recruited to promoters in a cell type-specific manner and can in turn associate with different protein partners so as to exert diverse biological effects (7). NFI is thought to be involved in the down-regulation of *CYP1A1* by oxidative stress and in the induction of *CYP2B* by phenobarbital (25, 26). NFI-binding sites are present in the regulatory regions of genes that are specifically expressed in the mammary gland (12), pituitary (22), thyroid (27), and olfactory neurons (14, 15). Our data indicate that NFI isoforms also regulate the expression of

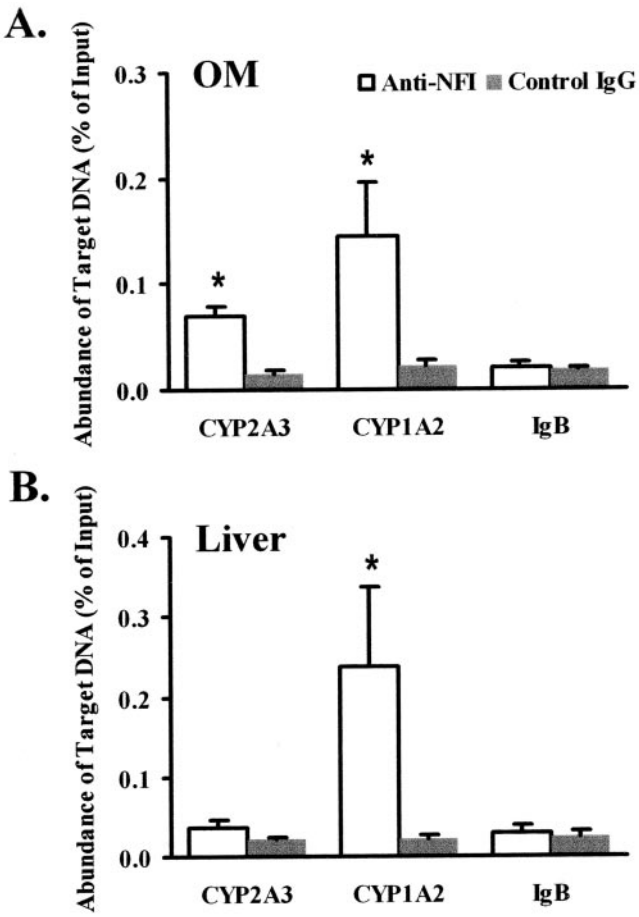

FIG. 5. **Tissue-selective association of NFI with *CYP2A3* promoter *in vivo*.** ChIP assays were performed as described under "Experimental Procedures." NFI-bound chromatin in the OM (*A*) and liver (*B*) of adult Wistar rats was immunoprecipitated with the H300 anti-NFI antibody. Normal rabbit IgG was used in place of the anti-NFI for negative controls. Enrichment of *CYP2A3*, *CYP1A2* (as a positive control for liver expression), and IgB (as a negative control) promoters in the immunoprecipitates was determined by real time quantitative PCR, which was conducted in duplicate, using primers specific for each promoter. The relative abundance of a specific promoter fragment (target DNA) was expressed as the percentage of total input chromatin. The results shown (means ± S.D.) represent data from four independent experiments. *, significantly greater than control; $p < 0.01$.

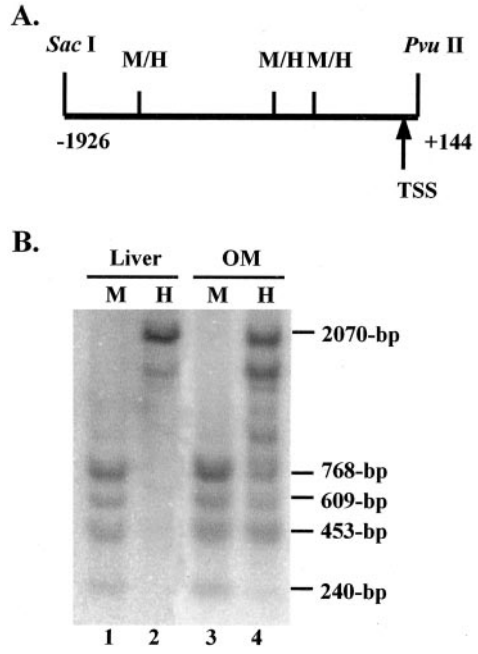

FIG. 6. **Tissue-selective methylation at the *CYP2A3* promoter.** Methylation status of the *CYP2A3* promoter (−1926 to +144, as a SacI-PvuII fragment) in the liver and OM of adult rats was analyzed by comparison of profiles of restriction fragments generated with MspI and HpaII (methylation-sensitive). *A*, location of MspI/HpaII (*M*/*H*) sites in the *CYP2A3* promoter region. The approximate position of the *CYP2A3* transcription start site (*TSS*) is shown. *B*, SacI/PvuII double-digested genomic DNA was further treated with MspI (*M*) or HpaII (*H*). Restriction fragments were detected on Southern blots, using the SacI-PvuII *CYP2A3* promoter fragment as a probe. The positions of the intact SacI/PvuII fragment (2070-bp) and four smaller fragments resulting from complete digestion by MspI or HpaII (240, 453, 609, and 768 bp) are indicated.

CYP2A3; this gene is expressed in the non-neuronal cells, including the sustentacular cells and cells of the Bowman's gland (4), in rat OM.

Multiple NFI isoforms are generated through extensive alternative splicings of the four NFI genes (21). For example, in rats, NFI-A2 differs from NFI-A1 in having a unique exon 1 (14, 16). The newly identified rat NFI-A splicing variant, NFI-A-short, is spliced to a new exon after a common exon 5. The resulting protein maintains the DNA binding and dimerization abilities but loses most of the transactivation/repression domain. By forming heterodimers, NFI-A-short can attenuate the effect of NFI-A2, and presumably any other NFI isoforms, thereby providing a mechanism for fine-tuning the expression of a target gene. A truncated splicing variant of NFI-B (human NFI-B3) had also been identified and had been shown to inhibit transactivation by other NFI factors in a previous study (28). Notably, although NFI-A2 and NFI-A-short mRNAs account for less than 3% of total NFI-A transcripts in adult OM, it is possible that they are enriched in certain cell types, where they could have significant roles in transcriptional regulation.

In a search for NFI clones in a rat OM cDNA library, Baumeister *et al*. (14) found that NFI-A was the most abundantly represented among identified NFI clones. This finding is in line with our observation, at the protein level, that NFI-A is the most abundant isoform in the OM. However, the other NFI proteins are also present in the OM and can potentially interact with the NPTA element, due to the high homology in the DNA-binding domain among all NFI proteins. In that regard, although our data clearly indicate a positive role for NFI in the regulation of *CYP2A3* expression, it was not possible to definitively identify the specific NFI isoforms that associate with the *CYP2A3* promoter *in vivo*. We believe that multiple NFI isoforms are functional at the *CYP2A3* promoter, a notion supported by our preliminary finding in an *Nfi-a* knockout mouse model (11), that *Cyp2a5* expression in the OM was not decreased in the absence of NFI-A.[2] However, individual NFI isoforms may have differing abilities to activate the *CYP2A3* promoter, partly as a result of their differing abilities to recruit or to interact with other transcription factors in the transcription complex (7) or to cooperate with co-activators (29, 30). Thus, for a better understanding of the mechanism of the involvement of NFI, it will be necessary to identify the NFI isoforms, as well as the proteins that interact with them at the *CYP2A3* promoter, in both neuronal (no *CYP2A3* expression) and non-neuronal (abundant *CYP2A3* expression) cells in the OM.

The mechanism underlying the absence of *CYP2A3* expression in the liver has yet to be determined. Although NFI transcription factors are found to be negative regulators in some cases, for example in the silencing of the glutathione transferase P gene (31), our data do not support a direct involvement of NFI in the hepatic silencing of *CYP2A3*. In the liver, NFI was found to be

[2] G. Ling, R. M. Gronostajski, and X. Ding, unpublished observations.

associated with promoters of transcriptionally active *CYP1A2* and with transcriptionally competent *CYP2B2* at uninduced state (26). However, under our ChIP assay condition, we did not detect significant association of NFI with *CYP2A3* promoter in liver chromatin. This finding suggested that the NPTA element was not accessible to NFI in the liver, possibly due to a transcriptionally silent chromatin structure. It had been reported that the affinity of NFI for nucleosomal DNA is 100–300-fold lower than its affinity for free DNA (32). The presence of an inhibitory chromatin structure at the *CYP2A3* promoter in liver is supported by the results of our promoter methylation assays. Cytosine methylation of a gene promoter is known to be associated with heterochromatin and stable gene silencing (33). By using methylation-sensitive restriction enzymes and Southern blot assays, we demonstrated that there was a nearly complete cytosine methylation at selected sites of the *CYP2A3* promoter in liver, but only a partial methylation at these sites in the OM, a tissue containing both *CYP2A3*-expressing and non-expressing cells. However, factors responsible for the tissue-selective methylation status, and the associated silencing of *CYP2A3* in the liver, remain to be identified.

Methylated DNA mediates gene silencing by intervening in transcription factor binding and by recruiting proteins that alter chromatin structure (33). There is emerging evidence that DNA methylation plays a role in the transcriptional regulation of genes encoding drug metabolism enzymes (34–36). Nevertheless, how DNA methylation is involved in tissue-specific gene expression is not well understood. Several lines of evidence suggest that DNA methylation only affects inactive genes and renders the gene silencing irreversible (33). In a model proposed by Turker (37), active promoters occupied by transcription factors prevent the methylation from spreading, and a decrease in transcription potential may lead to the invasion of DNA methylation in the promoter region and eventually the stabilization of gene silencing. We propose that as yet unidentified tissue-specific transcription factors are responsible for the maintenance of an active *CYP2A3* promoter in rat OM, whereas in most other tissues, in the absence of these factors, the transcription potential of *CYP2A3* is too low to prevent the spreading of DNA methylation. The binding sites for these putative, tissue-specific factors are most likely located far upstream of the *CYP2A3* promoter, as suggested by the results of our recent transgenic mouse study (38). Thus, in transgenic mice that contain a full-length *CYP2A3* transgene, with 3.4 kb of 5′-flanking region and 1.5 kb of 3′-flanking region, the expression level of the transgene was very low, and the tissue profile of transgene expression mimicked that of mouse *Cyp2a5* rather than that of rat *CYP2A3* (38). These data suggest that more distal regulatory modules are required for the robust and tissue-specific expression of *CYP2A3*. Further efforts to identify these putative, distal regulatory modules and their binding proteins, the roles of these proteins in controlling methylation and chromatin structure at the *CYP2A3* promoter, and their potential interactions with putative NFI co-activators at the NPTA element are warranted.

Acknowledgments—We thank Drs. Laurence Kaminsky and Randall Morse for helpful discussions and Dr. Adriana Verschoor for reading the manuscript. We also gratefully acknowledge the use of the Biochemistry and Molecular Genetics Core facilities at the Wadsworth Center.

REFERENCES

1. Ding, X., and Kaminsky, L. S. (2003) *Annu. Rev. Pharmacol. Toxicol.* **43,** 149–173
2. Fernandez-Salguero, P., and Gonzalez, F. J. (1995) *Pharmacogenetics* **5,** S123–S128
3. Honkakoski, P., and Negishi, M. (1997) *Drug Metab. Rev.* **29,** 977–996
4. Ding, X., and Dahl, A. R. (2003) in *Handbook of Olfaction and Gustation* (Doty, R. L., ed) pp. 51–73, Marcel Dekker, Inc., New York
5. Wang, H., Tan, W., Hao, B., Miao, X., Zhou, G., He, F., and Lin, D. (2003) *Cancer Res.* **63,** 8057–8061
6. Zhang, J., and Ding, X. (1998) *J. Biol. Chem.* **273,** 23454–23462
7. Gronostajski, R. M. (2000) *Gene* (*Amst.*) **249,** 31–45
8. Zhang, J., Zhang, Q.-Y., Guo, J., Zhou, Y., and Ding, X. (2000) *J. Biol. Chem.* **275,** 8895–8902
9. Chaudhry, A. Z., Lyons, G. E., and Gronostajski, R. M. (1997) *Dev. Dyn.* **208,** 313–325
10. Kannius-Janson, M., Johansson, E. M., Bjursell, G., and Nilsson, J. (2002) *J. Biol. Chem.* **277,** 17589–17596
11. das Neves, L., Duchala, C. S., Tolentino-Silva, F., Haxhiu, M. A., Colmenares, C., Macklin, W. B., Campbell, C. E., Butz, K. G., and Gronostajski, R. M. (1999) *Proc. Natl. Acad. Sci. U. S. A.* **96,** 11946–11951
12. Grunder, A., Ebel, T. T., Mallo, M., Schwarzkopf, G., Shimizu, T., Sippel, A. E., and Schrewe, H. (2002) *Mech. Dev.* **112,** 69–77
13. Steele-Perkins, G., Butz, K. G., Lyons, G. E., Zeichner-David, M., Kim, H. J., Cho, M. I., and Gronostajski, R. M. (2003) *Mol. Cell. Biol.* **23,** 1075–1084
14. Baumeister, H., Gronostajski, R. M., Lyons, G. E., and Margolis, F. L. (1999) *Brain Res. Mol. Brain Res.* **72,** 65–79
15. Behrens, M., Venkatraman, G., Gronostajski, R. M., Reed, R. R., and Margolis, F. L. (2000) *Eur. J. Neurosci.* **12,** 1372–1384
16. Xie, Y., Madelian, V., Zhang, J., Ling, G., and Ding, X. (2001) *Biochem. Biophys. Res. Commun.* **289,** 1225–1228
17. Kudrycki, K., Stein-Izsak, C., Behn, C., Grillo, M., Akeson, R., and Margolis, F. L. (1993) *Mol. Cell. Biol.* **13,** 3002–3014
18. Wells, J., and Farnham, P. J. (2002) *Methods* **26,** 48–56
19. Osano, K., and Ono, M. (2003) *Eur. J. Biochem.* **270,** 2532–2539
20. Frank, S. R., Schroeder, M., Fernandez, P., Taubert, S., and Amati, B. (2001) *Genes Dev.* **15,** 2069–2082
21. Grunder, A., Qian, F., Ebel, T. T., Mincheva, A., Lichter, P., Kruse, U., and Sippel, A. E. (2003) *Gene* (*Amst.*) **304,** 171–181
22. Norquay, L. D., Yang, X., Sheppard, P., Gregoire, S., Dodd, J. G., Reith, W., and Cattini, P. A. (2003) *Mol. Endocrinol.* **17,** 1027–1038
23. Futscher, B. W., Oshiro, M. M., Wozniak, R. J., Holtan, N., Hanigan, C. L., Duan, H., and Domann, F. E. (2002) *Nat. Genet.* **31,** 175–179
24. Carr, B. A., Wan, J., Hines, R. N., and Yost, G. S. (2003) *J. Biol. Chem.* **278,** 15473–15483
25. Morel, Y., and Barouki, R. (1998) *J. Biol. Chem.* **273,** 26969–26976
26. Kim, J., Min, G., and Kemper, B. (2001) *J. Biol. Chem.* **276,** 7559–7567
27. Ortiz, L., Aza-Blanc, P., Zannini, M., Cato, A. C., and Santisteban, P. (1999) *J. Biol. Chem.* **274,** 15213–15221
28. Liu, Y., Bernard, H. U., and Apt, D. (1997) *J. Biol. Chem.* **272,** 10739–10745
29. Chaudhry, A. Z., Vitullo, A. D., and Gronostajski, R. M. (1999) *J. Biol. Chem.* **274,** 7072–7081
30. Leahy, P., Crawford, D. R., Grossman, G., and Gronostajski, R. M. (1999) *J. Biol. Chem.* **274,** 8813–8822
31. Osada, S., Daimon, S., Ikeda, T., Nishihara, T., Yano, K., and Ymagawa, M. (1997) *J. Biochem.* (*Tokyo*) **121,** 355–363
32. Blomquist, P., Li, Q., and Wrange, O. (1996) *J. Biol. Chem.* **271,** 153–159
33. Bird, A. (2002) *Genes Dev.* **16,** 6–21
34. Nakajima, M., Iwanari, M., and Yokoi, T. (2003) *Toxicol. Lett.* **144,** 247–256
35. Lin, X., and Nelson, W. G. (2003) *Cancer Res.* **63,** 498–504
36. El-Osta, A., Kantharidis, P., Zalcberg, J. R., and Wolffe, A. P. (2002) *Mol. Cell. Biol.* **22,** 1844–1857
37. Turker, M. S. (2002) *Oncogene* **21,** 5388–5393
38. Su, T., Zhang, Q.-Y., Zhang, J., Swiatek, P., and Ding, X. (2002) *Drug Metab. Dispos.* **30,** 548–552